JOINT EUROPEAN TORUS JET

JET–P(93)09

J. Jacquinot

Summary on Tokamak Experiments, Heating and Current Drive

Summary on Tokamak Experiments, Heating and Current Drive

J. Jacquinot

JET-Joint Undertaking, Culham Science Centre, OX14 3DB, Abingdon, UK

Preprint of a paper to be submitted for publication in the proceedings of the
1992 IAEA Conference: Summary Talks.
February 1993

JET-P(93)09

Summary on Tokamak Experiments, Heating and Current Drive

J Jacquinot.

JET Joint Undertaking, Abingdon, Oxon, OX14 3EA, UK.

Preprint of a paper to be submitted for publication in the proceedings of the 1992 IAEA Conference: Summary Talks.

February 1993

I INTRODUCTION

When participants met at the conference, they were fully aware of 2 major pieces of news, a) JET had performed successfully a first Tritium injection experiment, and b) the world wide ITER engineering design activities had started. It is clear that such outstanding results would not have been possible without the knowledge acquired from the world's Tokamak experimental programme. Considering the huge amount of material presented at this meeting it is now a frightening task to summarize these results. There were 68 papers directly involved with tokamak confinement experiments. In addition 17 papers were dealing with heating and current drive and 5 papers came from other sessions. In total this summary draws its substance from 90 papers a number to be compared to a total of 225 papers in this conference.

Origin	Tokamak	Work Area	Newcomers
Brazil	TBR-1	Ergodic Limiter	
Canada	T de V, STOR-M	Biased Divertor	
China	HT-60B, HL1	Biased Electrode	
Czech.	CASTOR-1	Edge Turb. Biasing	
Europe	JET	D-T Operation Full Programme	
France	TORE-SUPRA	Super Cond. Coils	
Germany	ASDEX-U, TEXTOR	Divertor/First Wall	ASDEX-U
Hungary	MT-1M	MHD	MT-1M
India	ADITYA, SINP	Edge Turbulence	ADITYA
Italy	FT-U	7.5 T	
Japan	JT-6OU, JFT-2M, JIPP-IIU, TRIAM-1M, WT-3	Full Programme	JT-60U
Netherlands	RTP	ECRH	
Russian Fed.	TSP, T-10, TUMAN-3	Super Cond. Coil, ECRH	TSP
Spain	TJ-I	Fluctuations	
Switzerland	TCV	High Elongation	TCV
UK	COMPASS, START	Tight Aspect ratio	START
U.S.A.	TEXT, PHAEDRUS-T, MTX, TFTR, CDX-U, DIIID, PBX	Full Programme	
17	34		7

Table 1: A List of Operating Tokamaks Represented at the Conference

Table 1 gives the work area of the 34 tokamaks from 17 countries which are mentioned in the papers. The studies are performed with a large range of toroidal field (up to 7.5 teslas), size, current, aspect ratio and shape. Generally the smaller tokamaks contribute with information on turbulence and plasma behaviour relevant to edge plasma conditions found in larger tokamaks. There is a marked trend towards advanced divertor concepts and towards various active means of controlling the current profile. A number of new devices have come into operation since the last IAEA meeting and in order to welcome the newcomers it is a pleasure to show photographs of plasma obtained in 2 new devices. START (Fig 1a) has obtained results relevant to a tight aspect ratio geometry and ASDEX-U (Fig 1b) is a large divertor device conceived with a reactor relevant design. H-modes have been obtained in ASDEX-U very soon after initial operation ("noblesse oblige").

II BACKGROUND

Experimental research is inspired by competing concepts for a possible tokamak reactor and its underlying physics. To illustrate this point, let me consider 2 different ignited tokamak reactors.

i) **Reactor A** would use only inductive current drive in order to avoid operating systems which may have a large impact on the recirculating power. Therefore it would be semi-continuous; every few hours, it would have to stop for a few minutes to recharge the transformer. It would have to be re-ignited at the beginning of each new cycle using a short burst of heating. Running without the benefit of profile control, one has to dimension the reactor to ignite in L-mode, eg $R \sim 8$ m, $a \sim 3$ m, $B_\phi \sim 6$ T and $I_p \sim 30$ MA. P-H Rebut has described such a device emphasizing the simplicity, the cost advantages and important aspects of impurity retention. Several new results presented in Würzburg are pertinent to this mode of operation (AC operation, L-mode scaling, etc).

ii) **Reactor B** would be continuous using a significant amount of non-inductive current drive power. The relatively poor efficiency of current drive schemes forces to rely heavily on a large bootstrap contribution to the total current (more than 60 %). This means operating at high values of β_p (1 to 2) and controlling the current profile to avoid MHD instability. Typically this reactor operates with lower current ($\sim$ 15 MA) and high field ($\sim$ 8 T). It is a

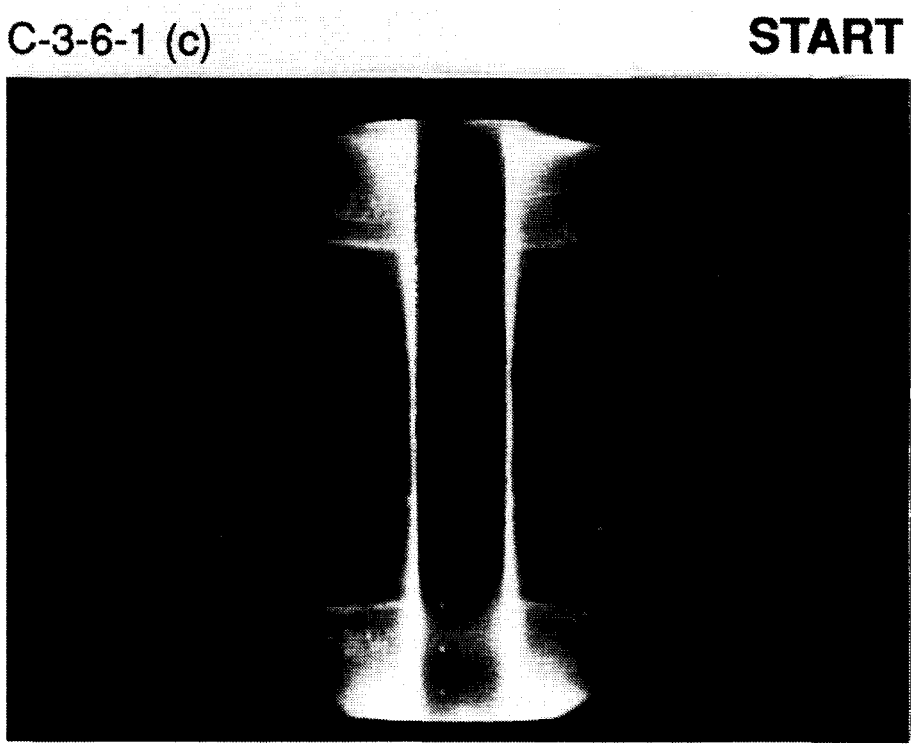

Fig 1a: Photograph of the plasma produced in START which recently came into operation. This is a tight aspect ratio machine which operates with natural elongation, $k \leq 2$.

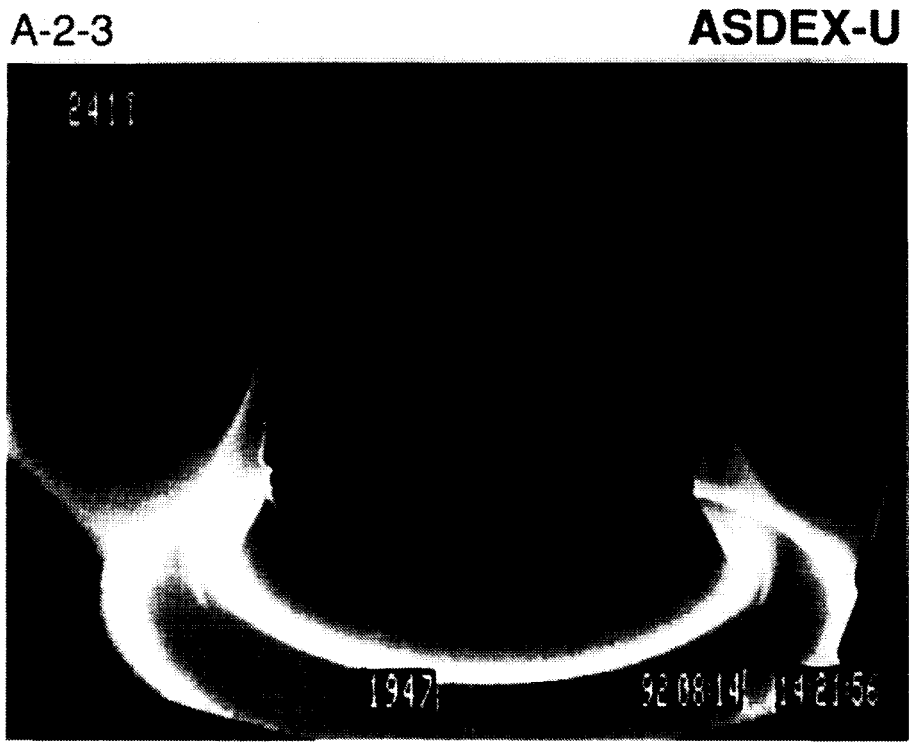

Fig 1b: Photograph of the plasma produced in ASDEX-U which also recently came into operation. The machine is designed to operate with a reactor relevant divertor.

trademark of this conference that operating at high β_p does provide the expected bootstrap current and more surprisingly gives rise to good normalised confinement. However, steady-state operation has not been demonstrated.

In all reactor concepts, power and particle exhaust must be provided by a **divertor**. The physics of the plasma in the divertor and the requirement on pumping and plasma facing components now appear as major issues.

Transport studies continue to attract much attention. The wind-tunnel approach to heat diffusion provides a physics basis to scale to reactor dimensions. Perhaps even more important is the condition on the ratio of particle to energy confinement time $\tau_p/\tau_E \leq 8$ which is required to prevent poisoning by helium ash accumulation. Ash poisoning would also occur if the average plasma temperature $< T > \geq 17$ keV. Poisoning arises from an excessively large slowing down time of the alpha particles[1].

III PROGRESS IN TECHNOLOGY AND PLASMA ENGINEERING

Reliable operation at high current without disruption has made considerable progress. The highest plasma current reached 7 MA in JET and the plasma was heated with up to 28 MW of additional heating power. MHD activity during the current rise is avoided by careful programming of the plasma aperture to prevent crossing low rational values of q_ϕ (Figs 2a and 2b). In several cases, the plasma inductance (TORE SUPRA; JET) is also controlled using LHCD. In DIII-D error fields are compensated to allow operation at low density. Large machines (JT-60U, JET etc) have developed disruption control devices which detect a disruption precursor and then acts on the elongation or other parameters to stop further development. However, there is at present no cure for some very fast disruptions occurring for instance at high β_p values.

TORE SUPRA and Triam-IM have demonstrated that a tokamak operating with superconducting TF coils could operate reliably at its nominal performance and have made progress towards operation in steady state.

Plasma facing components and first wall conditioning are key elements for tokamak operation. Thin layer coatings with beryllium, boron, silicon and

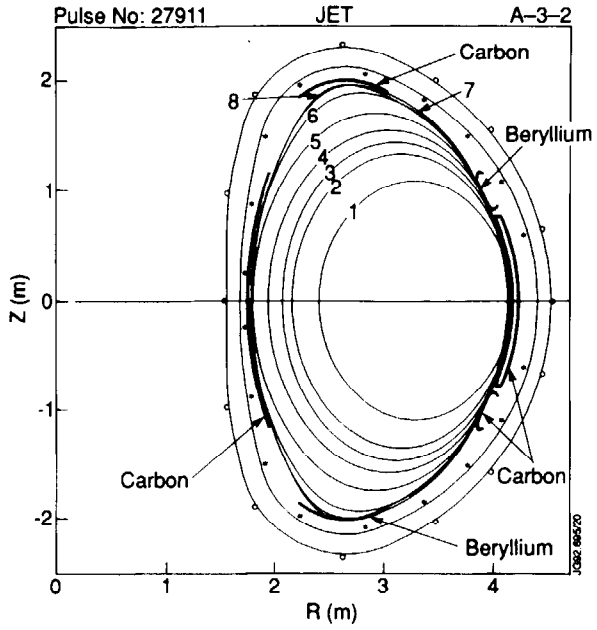

Fig 2a: Sequence of aperture increase during the rise to a 7 MA plasma in JET; numbers refer to time slices indicated in Fig 2b.

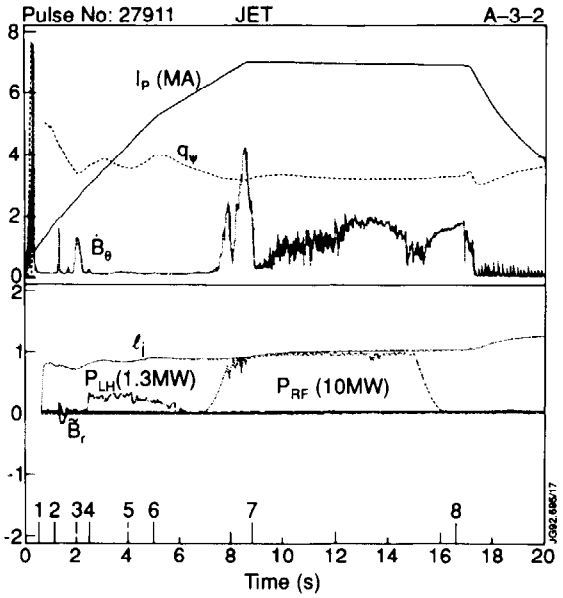

Fig 2b: Current, magnetic fluctuations, internal inductance LHCD and ICRH powers during a 7 MA plasma in JET, LHCD is used to save volt-seconds. The elongation is ramped down if a disruption precursor is detected (none in this case).

Lithium have been effective in reducing impurity content, in particular oxygen, and reducing particle recycling from the walls. Such wall preparations are a prerequisite to obtaining high performance modes such as the hot ion H-mode or the VH-mode. Limiters and divertor target tiles are, in all high performance devices, made of low Z material. CFC composite material offer the highest power loading limit to date. Extreme accuracy (± 0.5 mm) in the positioning of the tiles is required in order to achieve an acceptable power loading. Such accuracy has been instrumental in extending the operating range of TFTR. Nevertheless, the carbon bloom may still occur being triggered by a local instability (TORE SUPRA). The use of ergodic fields to spread the power load on the tiles has started to be used in JT-60U and TORE SUPRA and the observed trends are encouraging.

We note that active cooling of limiter tiles and divertor target plates are rarely used in large machines. This certainly reveals the high amount of risk attached to the fundamental requirement to locate the active cooling channel some 3 mm away from the high heat load. It should however be stressed that such a difficulty must be faced sooner rather than later en route to the reactor.

IV PEAK PERFORMANCE

The highest peak triple fusion products $n_D\tau_E T_{io}$ are listed in Table 2. The plasma stored energy W may not be in stationary state at peak performance and the definition of $\tau_E = W/P_{loss}$ where $P_{loss} = P_{in}$ - dW/dt can be reduced by as much as 30 % compared to P_{in}. The most notable progress since the last meeting comes from Japan and from DIII-D. In all cases, the peaked performance is obtained with a plasma current smaller than the maximum allowed by technical limits. The safety factor is moderate ($q_{95} \geq 4$). Except for the pellet enhanced phase PEP (JET) which is obtained in an ICRH-dominated discharge, these regimes are heated by NBI which provides power in the form of ion heating in the centre. Sawteeth are stabilised possibly by the fast ion pressure and very high central temperatures are reached. $T_{io} \sim 38$ keV in JT-60U (Fig 3). The electron temperature lags behind $T_{eo} \leq 12$ keV in NBI-heated discharges. In the PEP, it can reach 15 keV with $T_e \sim T_i$. In JET, the equivalent D-T fusion power corresponds to $Q \leq 1$ with, except in the PEP, more than half of the yield originating from beam-plasma reactions.

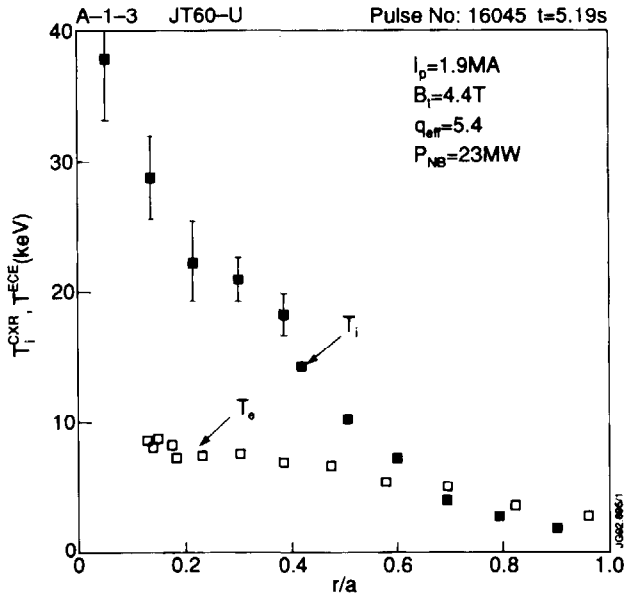

Fig 3: Ion and electron temperature profile during a high β_p discharge in JT-60U.

	$n_d \tau_E T_{io}$ (keV m^{-3} s)	COMMENTS	DURATION (s)
JET	$9\ 10^{20}$	Hot ion H-mode (3 MA)	1.5
	$7\ 10^{20}$	PEP (3 MA, ICRH)	1
JT-60 U	$4.4\ 10^{20}$	Hot ion; $\beta_p \simeq 1.6$ (1.66 MA)	0.8
	$2.2\ 10^{20}$	H-mode (2.7 MA)	
TFTR	$3\ 10^{20}$	Super-shot (hot ion)	0.5
DIII-D	$2\ 10^{20}$	VH-mode (1.6 MA)	0.5

Table 2: Peak triple fusion product $n_D \tau_E T_{io}$ achieved in several large tokamaks

The global energy confinement is excellent in these discharges. It exceeds 1 s in JET. In normalized form, all the 4 larger machines reach $\tau_E \sim 3$ to 4 $\tau_{EL\ mode}$. This is achieved with greatly reduced heat diffusivity in the plasma core $\chi_E \sim 1$–2 $m^2\ s^{-1}$ often combined with reduced diffusivity at the edge associated with the H-mode. In the VH mode, the size of the good confinement layer at the edge extends progressively inwards during the pulse.

V PROGRESS TOWARDS STEADY STATE

Complete steady state operation is a challenge for both engineering and for physics. As already mentioned, no faults are allowed from actively-cooled tiles which have to be thin in order to limit the tile surface temperature. On the physics side, the full current has to be driven non-inductively in steady state. Complete steady state has been achieved with LHCD in TRIAM-1M for 1 hour at a density of $n_e = 1.2\ 10^{18}\ m^{-3}$ or 3 minutes with $n_e = 2\ 10^{19}\ m^{-3}$. The steady state current does not exceed 50 kA. A mixture of ohmic and non-inductive current drive has been used in JET and TORE-SUPRA to extend the plasma current (up to 2 MA in JET) for over 1 minute. Here again the density did not exceed $2\ 10^{19}\ m^{-3}$ with $Z_{eff} \simeq 2$. In all the above cases, plasma confinement was L-mode.

Elmy H-mode with $\tau_E / \tau_{EL\ mode} \sim 1.4$ to 1.6 have been maintained for 18 s in JET. Special techniques are requested to obtain the appropriate rate of elm appearance

to control the density without excessive loss of energy confinement. They are based on plasma position control, gas puffing or energising an external coil producing a magnetic perturbation with a high m number (EML and ladder coils of JFT-2M).

Improved central confinement has also been reported in steady state using LHCD in TORE-SUPRA. A transition to a high central electron temperature is observed 1 s after application of the LHCD power. The improved central confinement which is maintained for 7 s (Fig 4) leads to an impressive central electron temperature. The control of the q profile is suggested as being responsible for the change of confinement (note that $V_{loop} \approx 0$): the magnetic shear is either very small or even reversed.

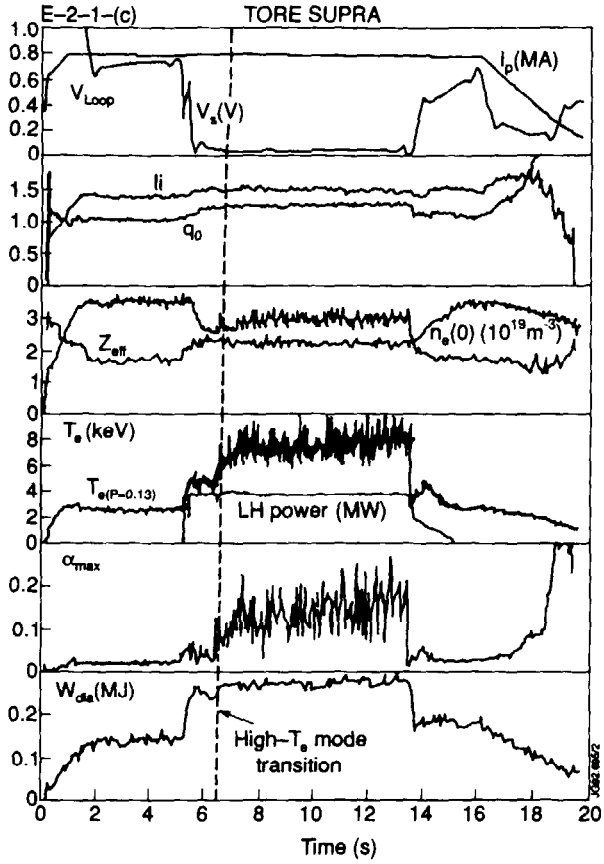

Fig 4: Traces during steady-state operation with enhanced central confinement in TORE SUPRA. LHCD drives the full tokamak current and the shear decrease or perhaps reverses in the good confinement zone.

In many experiments gettered walls provide adequate pumping rate to maintain constant density for up to 30 s. Active pumping results have been reported in TEXTOR, TOKAMAK de VARENNES and TORE-SUPRA.

VI GLOBAL ENERGY CONFINEMENT

The tokamak continues to be a paradise for imaginative experimentalists as energy confinement responds, quite often in an unexpected way to experimental procedures. The beneficial effects of a separatrix (H-mode), shear reversal (PEP) or edge recycling (super shot) are well established and confirmed by most experiments. This conference has added a substantial contribution to the importance of the current profile on confinement namely:

a) $\tau_E/\tau_{EL\,mode}$ increases with the internal inductance L_i. L_i values of up to 3.5 are obtained transiently with ramping the current down or changing the elongation or to a lesser extent by using LHCD. Fig 5 shows that the normalized

confinement increases almost linearly with L_i for both TFTR and DIII-D. A similar trend is observed in H-mode (DIII-D).

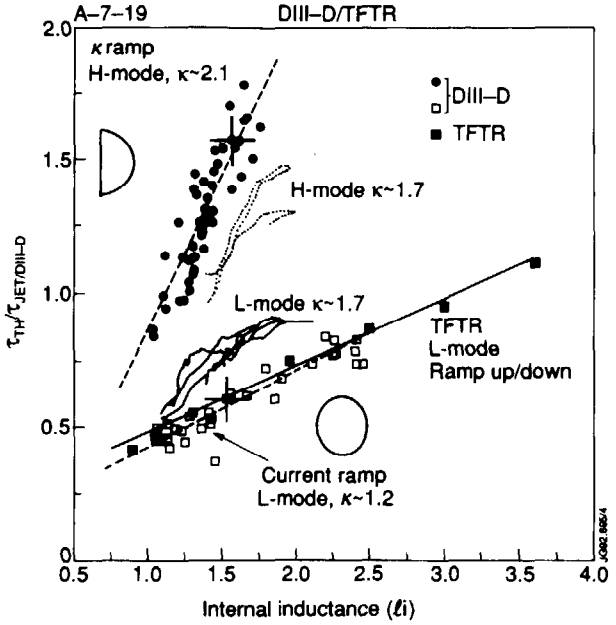

Fig 5: Normalised confinement versus internal inductance L_i in L mode (TFTR, DIII-D) and H-mode (DIII-D). The inductance is varied by changing rapidly the elongation or the plasma current. Warning the definition of L_i is likely to be different in the 2 machines!

b) $\tau_E/\tau_{EL\ mode}$ is also found to increase with the poloidal beta value (β_p). Since the bootstrap current fraction I_{BS}/I_p is proportional to β_p, such a result could also originate from a change of current profile which broadens with increased bootstrap current. Fig 6 combines results from JT-60 and JET which are similar despite the use of a different heating method. In the JET case, I_{BS}/I_P reached 0.7

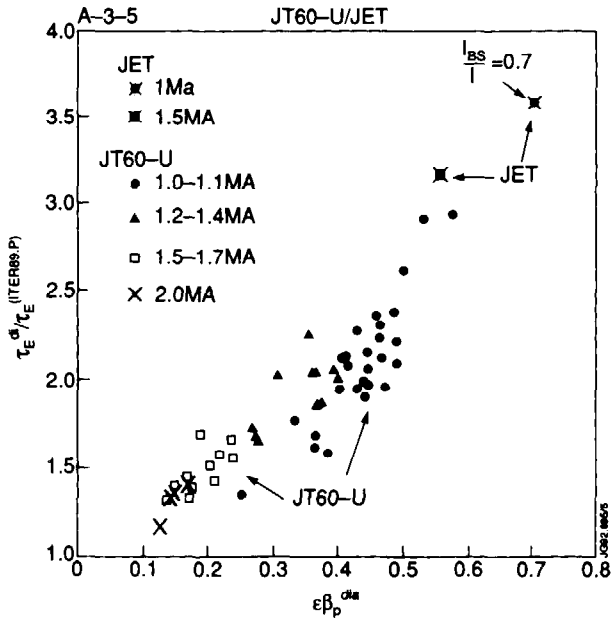

Fig 6: Normalised confinement versus $\varepsilon\beta$ for JT-60U and for JET. The same experiments show that the bootstrap current increases linearly with $\varepsilon\beta_p$ and reaches 70 % of the total current in the JET case.

c) Finally $\tau_E / \tau_{EL\ mode}$ is seen to increase with plasma triangularity (pulling the X-points towards the major axis). This effect combined with boronization allowed DIII-D to obtain the best performance of the VH-mode.

These results seem to indicate the beneficial role of the magnetic shear on the outer plasma region. However such an explanation is too simple to describe a complex behaviour. The importance of sheared poloidal flow of the plasma is now generally invoked. The correlation between reduced heat diffusivity and sheared flow is well established in the confinement barrier of the H-mode. It seems natural to generalise its influence to the entire plasma region; however a lack of adequate measurements prevents us from checking this assumption.

VII WIND TUNNEL APPROACH TO HEAT DIFFUSIVITY

The behaviour of scaled down model aeroplanes placed in a wind tunnel is routinely used to predict the performance of the full size model. It is important in the scaling down process and testing conditions to achieve the same dimensionless parameters occurring in the full size aircraft. Similarly, experiments have been performed in TFTR, JET, DIII-D keeping a number of dimensionless parameters at values expected in a reactor while changing only a

particular variable which needs to be extrapolated. The one fluid heat diffusivity χ is written as:

$$\chi = \chi_{Bohm}\, \rho^{*\alpha}\, F(\nu^*, \beta, q, s, T_e/T_i, ...)$$

with $\chi_{Bohm} \propto T/B$, $\rho^* \propto \sqrt{T}/Ba$. where ρ^* is the normalised Larmor radius and F is a functional form containing other dimensionless parameters which are kept constant. B is the magnetic field and a is the radial plasma dimension.

The value of α distinguishes between several types of turbulence responsible for anomalous confinement:

i) if $\alpha = 0$, long wavelength turbulence prevails; the wavelength is $\sim$ a. The diffusion is called "Bohm-like".

ii) if $\alpha = 1$, short wavelength turbulence dominates and the wavelength is $\sim \rho_i$ (the Larmor radius). The diffusion in this case is called "gyro-Bohm".

Experiments with ρ^* variation by a factor 2 to 3 gave clear indication that $\alpha \simeq 0$ and the large scale turbulence has been confirmed for the first time by measuring the wave spectrum in TFTR (Figs 7a and 7b) with beam emission spectroscopy.

Other variations of single dimensionless parameters have been performed (TFTR). They gave:

$\tau_E \propto A_i^{0.2}$	A_i = atomic number of the ion species
$\tau_E \propto \nu^{*0}$	ν^* = collisionality
$\tau_E \propto \beta^{0.5}$	β = normalised kinetic pressure

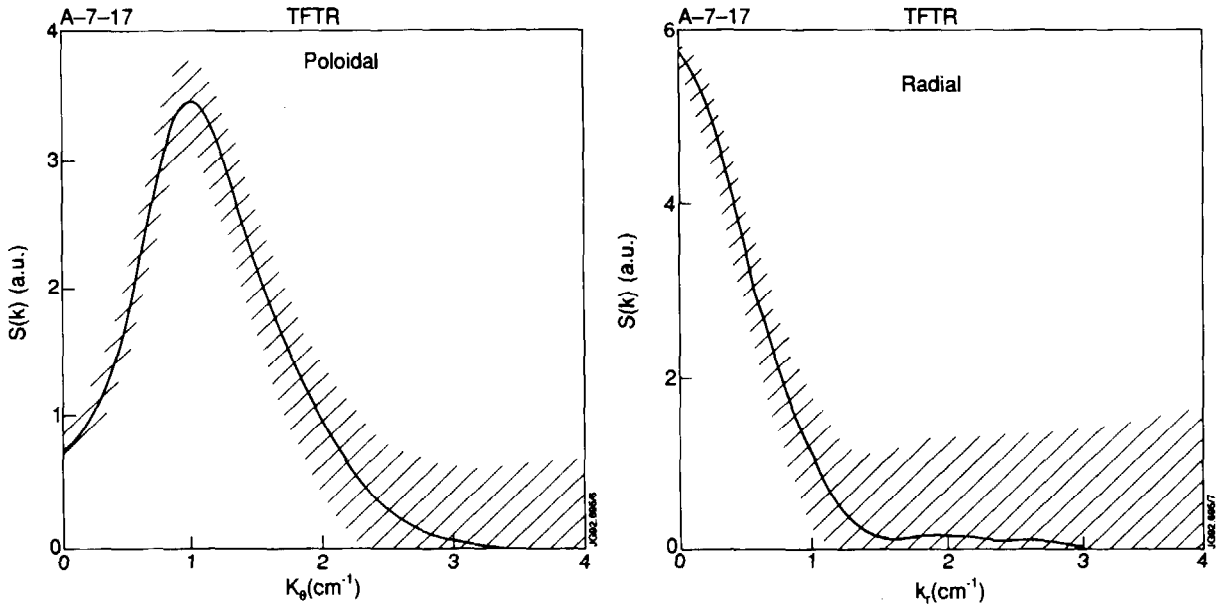

Fig 7: n_e turbulence spectrum for L-mode plasma in TFTR measured from Beam Emission spectroscopy ($r/a \sim 0.75$, $\rho_i \sim 0.14$ cm) in (a) the poloidal direction and (b) the radial direction. The fluctuations are dominated by long wavelength without wave-like structure in the radial direction.

Generally the observed behaviour are compatible with the ITER-P scaling $\tau_E^{ITER\text{-}P} \alpha \frac{T_e}{B} (\beta^2 \nu^*)^{1/4}$. However the β dependence seems to present a complex structure which will need to be clarified in future experiments. Other experiments (JET) highlight the diffusive character of heat transport and conclude to the absence of any inward heat pinch. Experiments in TEXT based on diffusion of energetic particles indicate that magnetic turbulence is not dominant.

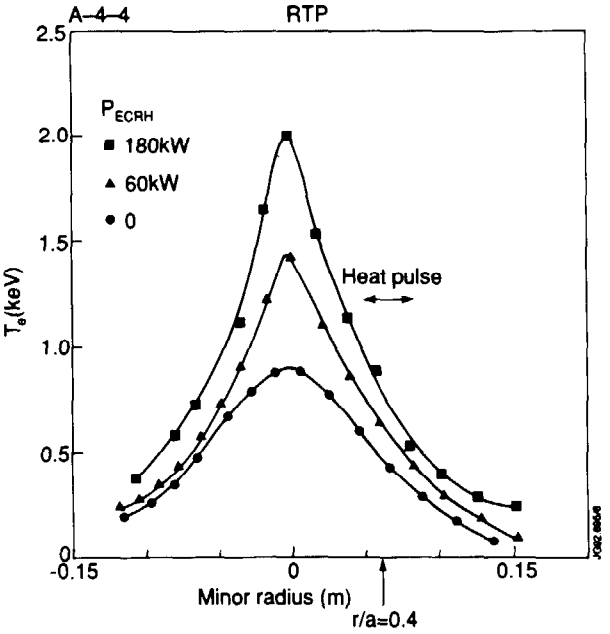

Fig 8: Temperature profile in RTP heated by ECRH. The incremental confinement time was found independent of T_e or of its variation.

It is interesting to note that the Rebut-Lallia-Watkins model which is based on the existence of a critical temperature gradient and is gyro-Bohm in its asymptotic limit matches imperfectly the ρ^* scaling results but continues to give a good representation

of experimental results obtained on many tokamaks in a wide range of conditions. In particular, the transport experiments performed with ECRH in RTP (FOM) measured using heat pulse propagation technique, showed that the incremental heat transport (τ_{inc}) was both independent of T_e and of the variation of T_e (Fig 8). τ_{inc} is calculated with the R-L-W model in its updated form as:

$$\chi \alpha \sqrt{\frac{T_e}{T_i + T_e}} \text{ instead of } \sqrt{\frac{T_e}{T_i}}$$

VIII H-MODE PHYSICS

New experiments using a magnetic brake in DIII-D support the leading idea that sheared $(E \times B)_\theta$ flow reduces the coherence length of turbulence across the lines of force and therefore reduces the amplitude and the effects of the turbulence. The sheared flow (gradient of E_r) is strongest at the edge (Figs 9a and 9b) at the location of the confinement barrier which develops during H-modes; it broadens during VH-modes. The quality of the confinement barrier is also associated with the appearance of a region of second stability regime and with the development of increased magnetic shear due to higher edge bootstrap current. Finally, it is noted that the large density gradient which builds up during the H-mode contributes to the edge electric field.

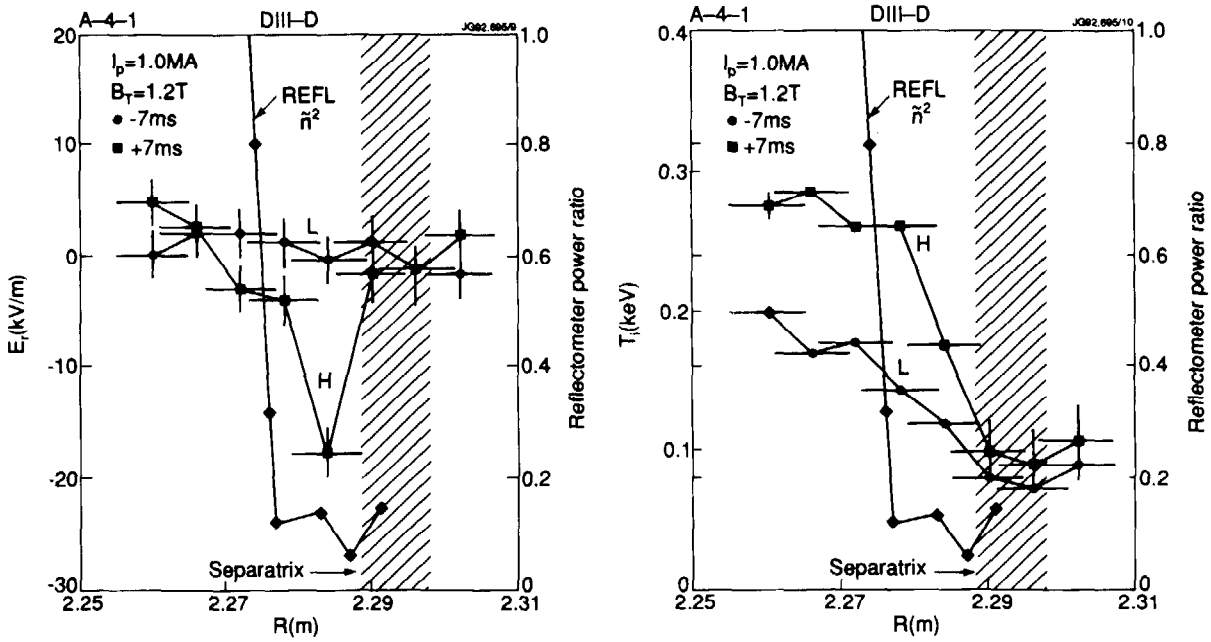

Fig 9: Variations of (a) the radial electric field E_r and density fluctuations, (b) ion temperature during L to H transitions in DIII-D . The results are consistent with sheared flow stabilisation of edge turbulence.

Following the original experiments by R Taylor and R Weynants, the plasma response to the electric field generated by a probe inserted in the plasma edge has been studied further on TEXTOR and HL-1. H-modes can be produced with both positive and negative biases. The amplitude and the profile of the radial electric field is observed to be governed by viscosity of the parallel plasma flow. Another originality of the TEXTOR experiment is to measure the particle confinement time (τ_p) which is seen to increase more than the energy confinement time after the H-mode transition. The increase of τ_p should be repeated on other devices since at present the τ_p/τ_E criteria mentioned in Section 2 seems to be out of reach in elm-free H-modes.

Finally, the conditions for H-mode transitions have now been characterised in numerous situations namely in TUMAN (pellet, gas, conditioning), JIPP II-U (ramp down of the current) and JFT-2M (Divertor bias). It is also possible to trigger ELMs with external magnetic perturbations (Fig 10) in order to control the density and the radiated power without excessive loss of energy confinement.

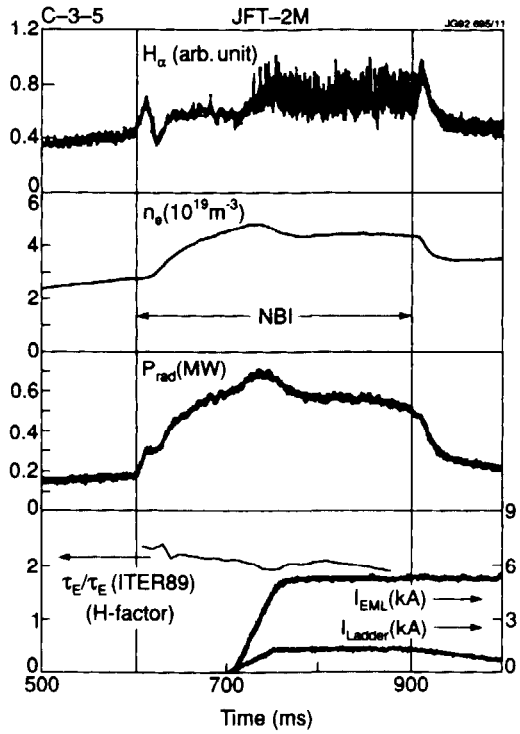

Fig.10: Control of the density rise and radiation by ELMs triggered with external magnetic field perturbations in JFT2-M.

IX CURRENT DRIVE

New results on current drive driven by **Lower Hybrid Waves** (LHCD) have been obtained in several experiments (HT-6B, PBX-M, JT-60U, TORE SUPRA, JET, TRIAM-1M, WT-3). The reality of the $k_{||}$ upshift has been demonstrated by measuring the onset of beam ion acceleration in JT-60U. The efficiency of current drive is seen to depend on the purity of the launched spectrum. Narrow spectra at low $k_{||}$ give the best results. The multijunction arrangement simplifies the task of phasing the waveguides, reduces the required number of windows and provides an increased range in plasma antenna coupling. Nevertheless, it is clear

that present structures are too complicated for a reactor environment. The use of a hyperguide to drive diffracting bars may provide the necessary simplification.

An important result is the **synergy between LHCD and ICRH** (low $k_{||}$ and minority hydrogen heating near the centre) which was reported by the JET team. The full plasma current (2 MA at $n_e \sim 2.5\ 10^{19}\ m^{-3}$) in JET can be driven in this way with an improved efficiency $\gamma \sim 0.45\ 10^{20}\ m^{-2}\ AW^{-1}$. The same method has been used to obtain long H-mode at 1 MA with zero loop voltage. The synergy is characterised by acceleration of the fast electrons to about 0.5 MeV, eg far beyond the energy obtained with LH only. The physics of the interaction remains to be resolved. The synergy between **ECRH and LHCD** has been demonstrated in WT-3 and agrees with theoretical expectations.

This meeting has hosted the first reports concerning current drive using the **fast waves** which are favoured in a reactor since they easily penetrate a dense large plasma core. The damping per pass for today's experiment is still weak. Nevertheless DIII-D has demonstrated a current drive efficiency which increases linearly with temperature (Fig 11) and agrees well with full wave codes. In JET, it was possible to stabilise or destabilise the sawteeth with travelling fast waves with the hydrogen minority resonance close to the sawtooth inversion radius. The effect on sawteeth is well modelled by the predicted dipole currents generated by ion current drive.

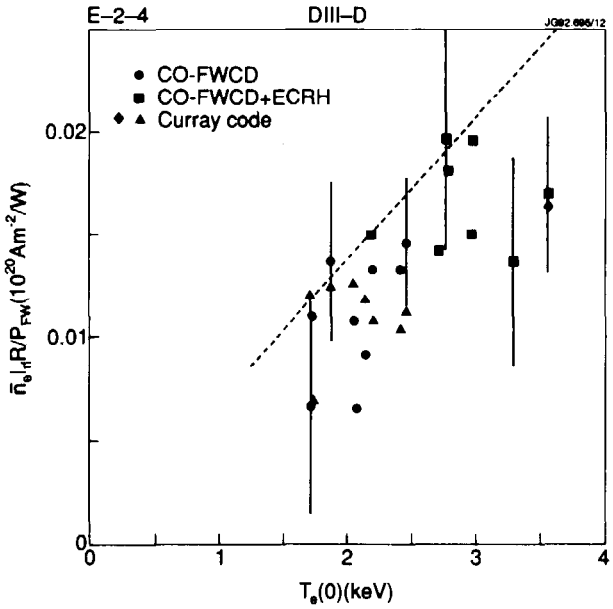

Fig 11: Efficiency of fast wave current drive (TTMP + ELD) in DIII-D versus central electron temperature and comparison to code calculations.

Helicity injection experiments have been performed in PPPL and in DIII-D where 30 kA and a plasma with $\varepsilon\beta_p \sim 1$ was sustained by helicity injection alone. It is also observed that a seed current can be generated spontaneously by transport alone.

In summary, good progress has been reported both on the physics and on the efficiency of current drive. New reactor relevant methods have been used. However we remark that the efficiency is still insufficient to drive a reactor with an acceptable level of recirculating power and that no current drive experiment operates in the reactor regime at $n_e \geq 10^{20}$ m^{-3}. We also note that current drive using Neutral Beam injection has never been performed in the super Alfvénic regime expected in a reactor; unstable gap modes are a potential threat for current drive generated by NBI.

X HEATING

The most important results is the use of Neutral Beam Injection (NBI) to inject tritons at 78 keV during the JET experiments. NBI fuelled a tritium concentration of 11 % with a gas fuelling efficiency of 5 %. Most of the unused tritium was condensed on the cryo-panels of the NBI pumps and could be recovered with nearly full efficiency.

Ion Cyclotron Resonance Heating (ICRH) is now a standard tool used for many physics experiments. The maximum coupled power has reached 22 MW. The complexity of plasma-antenna coupling is now alleviated by the use of automatic impedance matching and plasma positioning under feedback control. The physics of ICRH edge effects is now well based on the induction sheath rectification process. $K_{||}$ shaping, antenna geometry and the use of low Z screen materials (B_4 C and B_e) are used to eliminate deleterious effects. An antenna without screen tested in TEXTOR gave promising results and appears worth considering further as it would be simpler to operate in a reactor environment.

Electron Cyclotron Resonance Heating (ECRH) is performed using either gyrotrons or Free Electron Lasers (FEL). The Russian gyrotrons continue to lead the field with long pulse units capable of 400 kW at 140 GHz. Heat transport and the physics of ECRH have been studied in FOM. FEL has been used for the first time in MFTX delivering huge power spikes (1.4 GW, 20 ns). At this level, the absorption is highly non-linear. The experiments have verified the non-linear behaviour.

The conference also noted Ion Bernstein Wave Experiments at higher frequency (130 MHz) with good thermal ion heating in the plasma core (JIPPII-U) and the ambitious adiabatic compression project TSP which is progressing well in TROISK with particular attention to plasma wall interaction and with plans to inject tritium.

XI POWER AND PARTICLE EXHAUST WITH LIMITERS AND DIVERTOR

There is a general consensus in the tokamak community that the divertor is the most important issue to be solved en route towards a tokamak reactor. If divertor tiles would receive the full loss power of an ignited reactor, the tile power loading would exceed 40 MW m^{-2}; well in excess of acceptable levels (< 10 MW m^{-2}) which are compatible with the tile erosion rate and the reliability requested in a reactor. Several forms of advanced divertor concept are emerging, theygenerally involve a closed divertor with a large wetted area allowing impurity retention as well as radiation of most of the conducted power transmitted by the divertor channel. In a number of schemes, the diverted flux tube enters a slot geometry so that the neutralised particles are not re-emitted towards the main plasma. Modelling of the divertor channel is under active development in various groups. At this stage the models are still incomplete and a number of observations in DIII-D and JET remain to be explained. Nevertheless both theory and experiments agree that operation at low density is impossible for long pulses because the divertor temperature exceeds 20 eV leading to excessive sputtering from the tiles. Fortunately, the scrape off density rises sharply with the core density and impurity contamination is much reduced at high bulk densities (Fig.12).

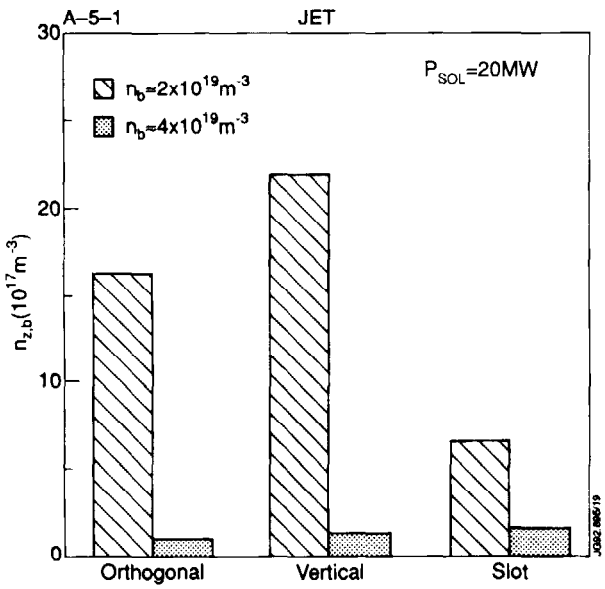

Fig.12: Calculations (JET) of bulk impurity density for various divertor geometry. The dominant parameter is the bulk electron density.

Consequently, reactor regimes acceptable for divertor operation can be found for central density values in the range of 2 to 3 10^{20} m^{-3}. The plasma is fuelled at the

periphery by gas and pellet injection maintaining a flat density profile. A plasma flow at high density in the divertor channel is used to radiate a substantial amount of the power. In JET, divertor plasma heated with 22 MW could be stably maintained in a high density regime with more than 90 % of the power radiated. This regime was obtained with the ion drift away from the target plates and with tiles made of beryllium. The plasma stayed in L-mode with, in some cases, a weak elmy behaviour. Gas injection was under feedback control to maintain a prescribed divertor tile temperature. Textor also obtained highly radiating plasmas using a limiter configuration and neon injection (under feedback control). It is remarkable in this experiment that the central neon concentration remained at acceptable levels. TORE-SUPRA demonstrated the efficiency of an ergodic divertor to radiate power and retain impurities.

In divertor experiments, it is important to avoid that the radiating marfe escapes the divertor region which then looses the capability to retain impurities.

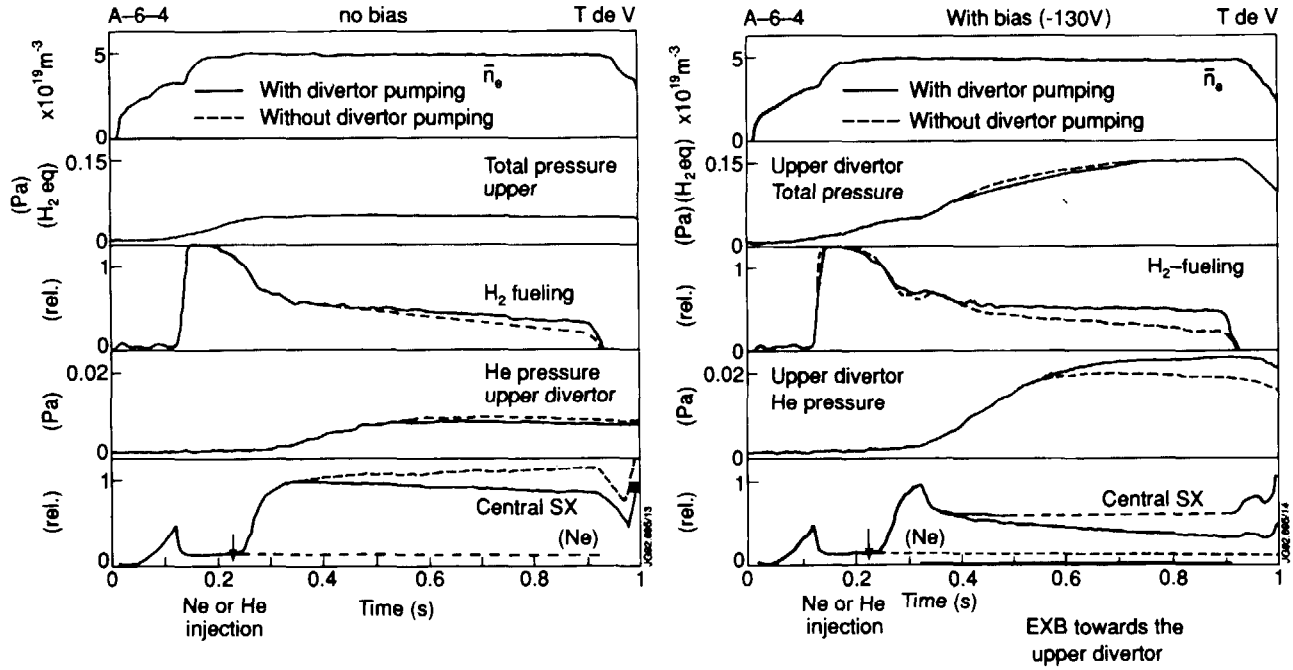

Fig 13: Divertor studies in Tokamak de Varennes with and without divertor pumping (a) without biasing; (b) with biasing. Removal of Neon or Helium is effective with the combination of pumping and biasing.

The second task of the divertor is to provide exhaust for the Helium resulting from D-T reactions as well as from impurites released by plasma facing components. It is important to concentrate the exhaust gas near the pump mouth in order to improve the pumping rate. Tokamak de Varennes has installed active pumping (cryogenic pumps) associated with divertor plate biasing

(Fig 13). Biasing (~ 130 V) was effective to increase, via E x B flow, the impurity outflow by a factor 2.5 and injected Neon and Helium were pumped with a time constant of about 0.5 s. It is clear that this type of experiment is still too sparse and that the reactor relevance of particle exhaust schemes ought to receive attention from an increasing number of devices.

XII OTHER REACTOR ISSUES

i) TAE Modes

Resonant interaction of global Alfvén gap modes with alpha particles is a potential threat for sustaining ignition in a reactor. The threshold for the instability is well described by theory. Experiments using NBI or ICRH in the minority regime have verified the linear characteristics of the instability. It is much less clear what will be the consequences of the instability on confinement of alphas. In DIII-D, up to 50 % of the NBI induced fusion yield is lost in the form of large bursts where $\beta_{fast} \sim 2\ 10^{-2}$. In TFTR, TAE modes induced by the toroidal precession of trapped orbits of minority ions created by ICRH (Figs 14a and 14b) led only to small losses. The DIII-D experiments demonstrated that the instability can be quenched by the development of a peaked current profile which induces damping via coupling to the Alfvén continuum.

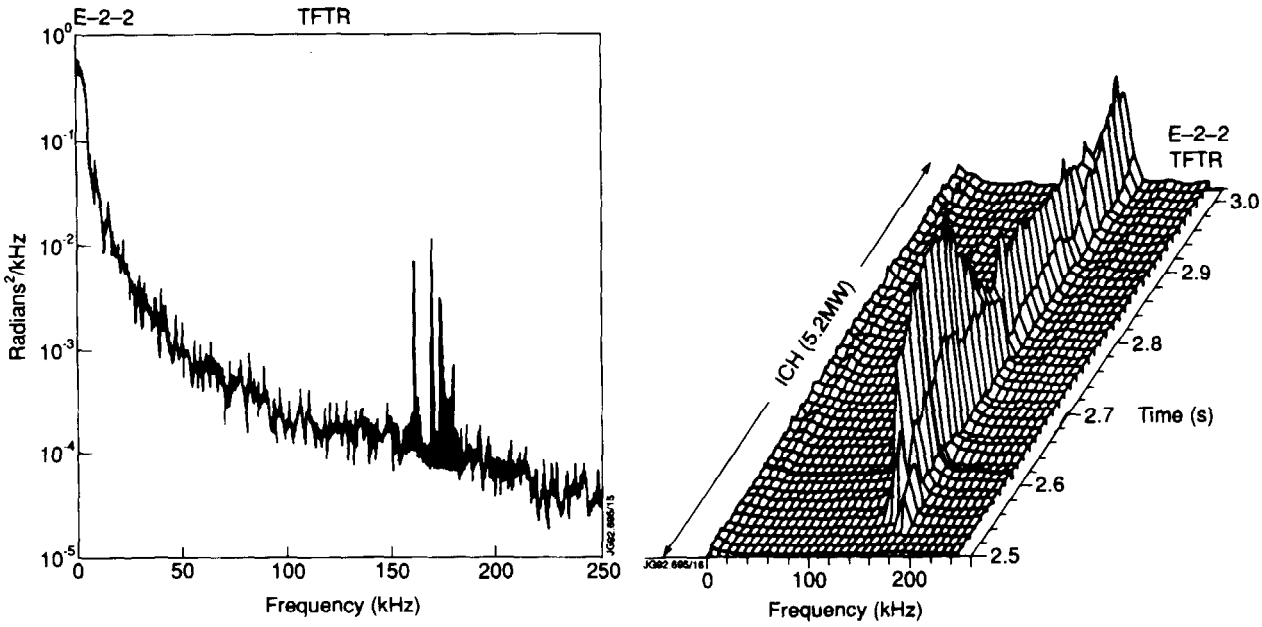

Fig 14: (a) TAE mode instability spectrum during ICRH heating in TFTR. The instability is driven by the fast particles accelerated by H minority ICRH (P > 3 MW); (b) Instability spectrum is shown as a function of time for a power level of 5.2 MW.

ii) AC Tokamak Operation

In support of the semi-continuous reactor scenario mentioned in Section 2, JET demonstrated a reliable reversal of the tokamak current and the establishment of a second current plateau (2 MA). The dwell time between the current quench and the following breakdown can be made short and the reversal phase (between 2 flat tops) could be completed in 5 s. No impurity deleterious effects have been observed. The requirement to operate ITER in the AC mode would imply the increase by 0.5 m of the transformer radius.

iii) Fast Ion Losses and Confinement Degradation due to Toroidal Field Ripples

JT-60U, TFTR and JET have reported new results on the effects of the toroidal ripple on fast particle losses and on confinement. In addition to first orbit losses, stochastic losses may occur for particles in the MeV range. The observed losses appear in line with theoretical predictions for stochastic losses of tritons (JET, TFTR) and ICRH induced fast ions (JET). However unexpected effects have been observed such as delayed losses (TFTR) or poor H-mode performance at high field ripple (JET, JT-60U). When JET is operated with 16 coils instead of the usual 32 coils, it is impossible to obtain an elm-free H-mode. The confinement is poor and the toroidal rotation is quenched. Similar effects are seen in JT-60U: High performance discharges are only obtained with smaller plasmas displaced on the high field side in order to avoid regions of high ripple. The physics mechanism for the degradation remains to be resolved. However, these results are a strong incentive to conceive ITER with a ripple well below the value that would be required to suppress the stochastic losses.

XIII OVERALL PROGRESS AND CONCLUSIONS

This IAEA conference will remain memorable being marked by the first tritium experiment and by considerable progress from a world wide experimental programme. Fig 15 illustrates the highest fusion yield achieved to date, it also shows that the next task ahead of us is to progress on the stationarity of the high yield operation. Fig 16 gives a global view of the progress in fusion power as the years go by. The JET results obtained with a Tritium/Deuterium ratio of 11 % will soon be surpassed by new progress from TFTR and JET. A fusion power in excess of 10 MW will appear within reach of the next 2 years when 50 % D/T

ratios will be used for the first time. ITER will produce 100 times more power and the burn time will need to be considerably extended. The extension of the pulse duration raises the most difficult challenge before the next IAEA conference. Meeting the challenge will imply placing the emphasis on edge and divertor physics, profile control and steady state operation using current drive, experimental and technical advances on power and particle exhaust. Finally, I have no doubt that transport physics will continue to fascinate many of us although our practical experience which has been earned the hard way appears nearly adequate to define the ignition regime.

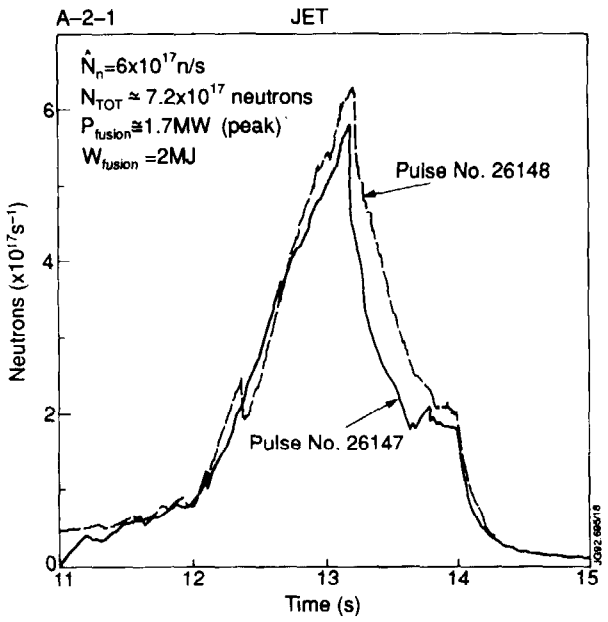

Fig 15: Neutron flux during the first 2 tritium shots (JET). The peak fusion power reached 1.7 MW. $n_T/n_D = 0.11$.

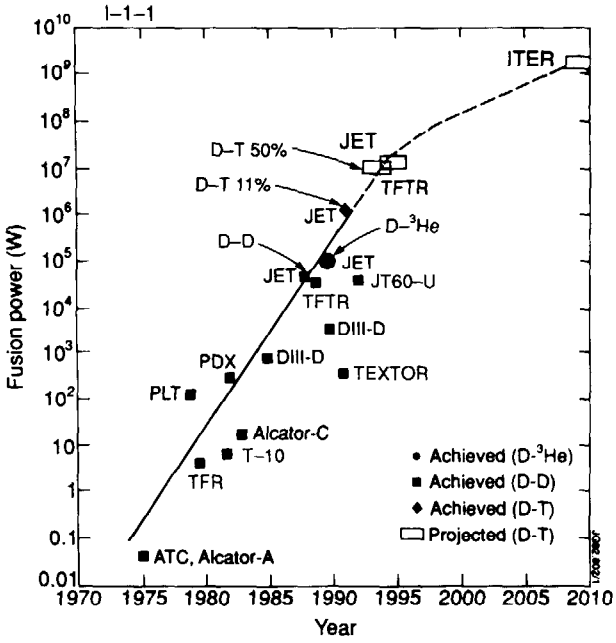

Fig 16: Histogram of fusion power in tokamaks and projected values.

ACKNOWLEDGEMENTS

It is a pleasure to acknowledge the valuable contributions of Dr V Bhatnagar in the preparation of this summary.

REFERENCES

[1] R. J. Bickerton, "Dynamics of a Steady-State D-T Burning Tokamak Plasma", JET-R(92)03.